



OPEN An integrated physics-guided machine learning approach for predicting asphalt concrete fracture parameters

Manzoor Elahi¹, Rawid Khan¹, Tufail Mabood¹, Muhammad Salman Khan^{2✉}, Awais Ahmed³, Mahmood Ahmad^{4,5} & Zsolt Tóth^{6✉}

Accurate prediction of fracture energy (G_f) in asphalt mixtures is important for durable asphalt pavements designing. Traditional experimental approaches are reliable but need resources, whereas numerical simulations, such as finite element models (FEM), offer flexibility but needs accurate input parameters and calibration. Recent advances in machine learning offer rapid prediction capabilities; however, interpretability and physical relevance remain challenging in this regard. This study presents a hybrid framework that integrates experimental Single Edge Notch Beam (SENB) tests, finite element simulations, and machine learning models to predict fracture parameters for asphalt mixtures. Experimental testing quantified fracture energy, while FEM simulations replicated the fracture response numerically. Machine learning models, including Linear Regression, Gradient Boosting, and AdaBoost, were trained on mixture properties such as stability, flow, air voids, and Stiffness Modulus at 20 °C (ITSM20) to predict surrogate fracture energy. A novel, dimensionally consistent surrogate equation was proposed to link key mixture properties to fracture energy, validated against both experimental and numerical results. The surrogate model demonstrated best accuracy with a mean relative error compared to experimental data. This novel integrated approach, adopted in this study, provides a practical and physics-guided methodology for rapid and reliable prediction of fracture behavior in asphalt mixtures, bridging experimental observations, numerical simulations, and data-driven machine learning modeling, and offering insights for mixture optimization and pavement design.

Keywords Fracture energy, Asphalt mixtures, Physics-guided machine learning, Surrogate modeling, Single-edge notched beam, Surrogate fracture parameters

Abbreviations

AC	Asphalt Content – % (by weight of mix)
CF	Coarse/Fine Ratio
D	Characteristic Beam Dimension (mm)
EffAC	Effective Asphalt Content % (by weight of mix)
FEM	Finite Element Method
Flow	Flow Value (mm)
G _f	Fracture Energy (N mm)
G _{mm}	Maximum Theoretical Specific Gravity
ITSM20	Indirect Tensile Stiffness Modulus at 20 °C (MPa)
ITSM30	Indirect Tensile Stiffness Modulus at 30 °C (MPa)
K	Scaling Constant

¹Department of Civil Engineering, Main Campus, University of Engineering and Technology, Peshawar 25000, Pakistan. ²College of Civil and Transportation Engineering, Shenzhen University, Shenzhen 518060, China. ³Department of Built Environment, Oslo Metropolitan University, Oslo, Norway. ⁴Institute of Energy Infrastructure, Universiti Tenaga Nasional, Kajang 43000, Malaysia. ⁵Department of Civil Engineering, University of Engineering and Technology Peshawar (Bannu Campus), Bannu 28100, Pakistan. ⁶Faculty of Wood Engineering and Creative Industries, University of Sopron, Sopron, Hungary. ✉email: msalman.khan0099@gmail.com; toth.zsolt@uni-sopron.hu

MAE	Mean Absolute Error (Target unit)
MAPE	Mean Absolute Percentage Error (%)
ML	Machine Learning
MSE	Mean Squared Error – (Target unit) ²
P4	Percent Retained on Sieve #4 (%)
P34	Percent Retained on 3/4" Sieve (%)
P38	Percent Retained on 3/8" Sieve (%)
P200	Percent Passing Sieve #200 (%)
R ²	Coefficient of Determination
RMSE	Root Mean Squared Error (Target unit)
SENB	Single Edge Notch Beam
SFR	Stability to Flow Ratio (Unitless)
Stab	Stability (N)
UWt	Unit Weight (kN/m ³)
Va	Air Voids (%)
Vis	Viscosity (Pa s)

The key understanding the fracture behavior of asphalt mixtures under mechanical loading, such as single edge notch beams is crucial for ensuring long-term pavement durability performance¹. Over the past decades, researchers have employed both experimental and numerical techniques in their researches, to investigate the mechanical and fracture properties of asphalt concrete^{2,3}. Tests in laboratories for material testing, such as the Single Edge Notch Beam (SENB) test, bending, and indirect tensile strength tests have been widely used to quantify fracture toughness, fracture energy, and load-deformation characteristics of asphalt mixtures^{4–7}. These experimental testing methods provide a quick and direct measurement of asphalt performance but are often take a lot of time, need resources, man power and limited in the number of mixtures and conditions that can be tested^{8–10}. Consequently, alternative approaches using numerical modeling, including finite element simulations, have gained traction, enabling researchers to predict fracture response under various loading conditions with reduced experimental effort^{11–13}. Finite element methods are extensively used by the researchers in their research studies, specially, those implemented in software such as ABAQUS, have been applied in a very extended way, to check and simulate the stress distribution and crack propagation in notched asphalt beams, which offering a flexible framework for investigating complex material behavior such as asphalt by using Prony series coefficients or using the cohesive zone modeling. These numerical models, however, depend heavily on accurate input parameters and material characterization, which often introduces uncertainty into predictions^{14–18}.

In parallel, the field of materials engineering has witnessed an interest, that is growing in machine learning (ML) and data-driven based methods to model material properties such as Asphalt^{19–22}. ML models have the capability to capture the most complex, nonlinear relationships between mixture constituents, mechanical properties, and fracture response of asphalt, without relying solely on explicit physical formulations^{22–24}. Few studies have applied algorithms in this advance filed simulation techniques, such as Linear Regression, Gradient Boosting, and AdaBoost to predict stiffness modulus, fatigue life, and rutting resistance in asphalt mixtures, demonstrating that data-driven approaches can complement experimental and numerical investigations in traditional laboratories. Yet, while these models provide rapid predictions, their interpretability and direct link to physical fracture parameters remain limited^{24,25}. This has led to the necessity of hybrid physics-guided ML approaches, where surrogate fracture parameters derived from measurable mixture properties such as stability, flow, air voids, and stiffness serve as ML targets and bridging experimental observations and numerical predictions with predictive modeling using machine learning techniques in detail^{26,27}.

Although there are substantial advancements, key research gaps are still present. Although there are substantial advancements, key research gaps are still present. First, few studies have integrated experimental, numerical, and machine learning approaches in a combined framework to systematically predict fracture energy and brittleness in asphalt mixtures^{26–29}. While some published ML-based studies have examined conventional performance indicators such as stiffness or rutting resistance, while direct prediction of fracture energy for notched beams through machine learning especially when coupled with hybrid physics-guided surrogates remains largely unexplored^{30,31}. Second, while surrogate fracture parameters have been conceptually proposed, there is a lack of practical formulations that are both dimensionally homogeneous and validated against experimental and FEM results^{30,31}. Lastly, there is limited discussion on validating ML-based surrogate predictions against both experimental and numerical benchmarks to quantify their accuracy and robustness^{32,33}.

This study addresses these gaps mentioned in the previous paragraph, by developing a hybrid framework that integrates experimental SENB tests (performed at university of engineering and technology Peshawar, Pakistan), FEM simulation with ABAQUS, and ML models to get the fracture toughness, use the predicted response in conjunction with the Python to further train on the dataset to predict surrogate fracture parameters in asphalt mixtures. Experimental work provides measured fracture response, FEM models simulate numerical behavior for the same specimens, and ML models including Linear Regression, Gradient Boosting, and AdaBoost predict surrogate fracture energy based on mixture constituents and mechanical properties. Overall, A novel surrogate fracture equation is proposed to link mixture properties (stability, flow, ITSM20, and beam dimension) to fracture energy, allowing a physically interpretable, dimensionally consistent prediction. This approach enables a rapid prediction of fracture energy without additional physical testing, followed by cross-validation against both experimental and numerical data, and exploration of parameter sensitivity to improve mixture design.

Methodology

This study was conducted through an integrated, multi-stage methodology shown in Fig. 1 designed to develop a physics-guided machine learning framework for predicting fracture energy of the Single Edge Notch Beam. It started with an experimental program involving Single Edge Notch Beam (SENB) tests on asphalt mixtures to obtain benchmark fracture energy values. Concurrently, the finite element method (FEM) simulations were developed and validated against the experimental results of force displacement curve, to generate numerical fracture energy. A comprehensive dataset of mixture properties was subsequently utilized for machine learning modeling to perform correlation analysis and train multiple machine learning models including Linear Regression, Gradient Boosting, and AdaBoost. The core of the framework involved the development of a novelty based, dimensionally consistent surrogate equation that synthesizes key mixture properties. At the final stages, the predictions from the surrogate model were validated against both experimental and numerical benchmarks to ensure accuracy and physical relevance. To clearly articulate this progression, Sect. 3 is structured to mirror the methodological sequence. Section 3.1 presents the experimental procedures and key fracture measurements that serve as the foundational reference. Section 3.2 then introduces the FEM model development and its validation using experimental force–displacement curves. Section 3.3 focuses on the derivation of the surrogate fracture equation, highlighting its dimensional consistency and its role in linking physical parameters to fracture energy. Finally, Sect. 3.4 describes the machine learning models trained using both raw mixture properties and the surrogate-derived parameters, followed by a comprehensive evaluation against experimental and numerical benchmarks.

Experimental program

The experimental program was designed to obtain precise data on the fracture behavior of asphalt concrete, which subsequently provided the foundation for finite element analyses and machine learning prediction. Single Edge Notch Beam (SENB) samples were made in a standard rectangular shape with dimensions of 375 mm in length, 75 mm in width, and 100 mm in height. To ensure a controlled crack initiation path, a middle notch of 19 mm depth was made at the center of each sample, as shown in Fig. 2. The aggregates used in this study were obtained from the KARKON Plant located near the Motorway Toll Plaza, with the source material originating from the Margalla region. These aggregates were selected to meet the National Highway Authority (NHA) Class

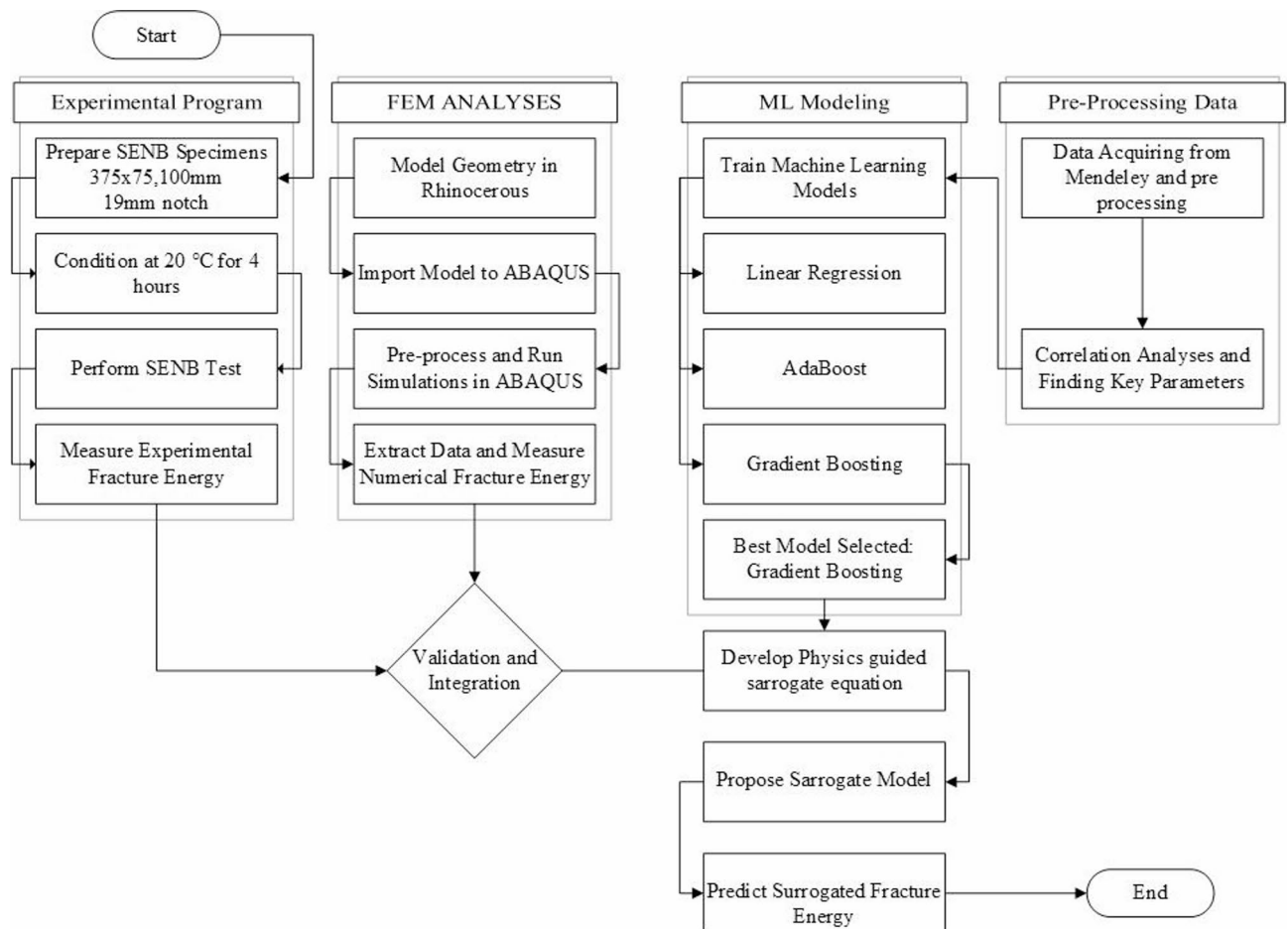


Fig. 1. Hybrid framework for predicting fracture energy.

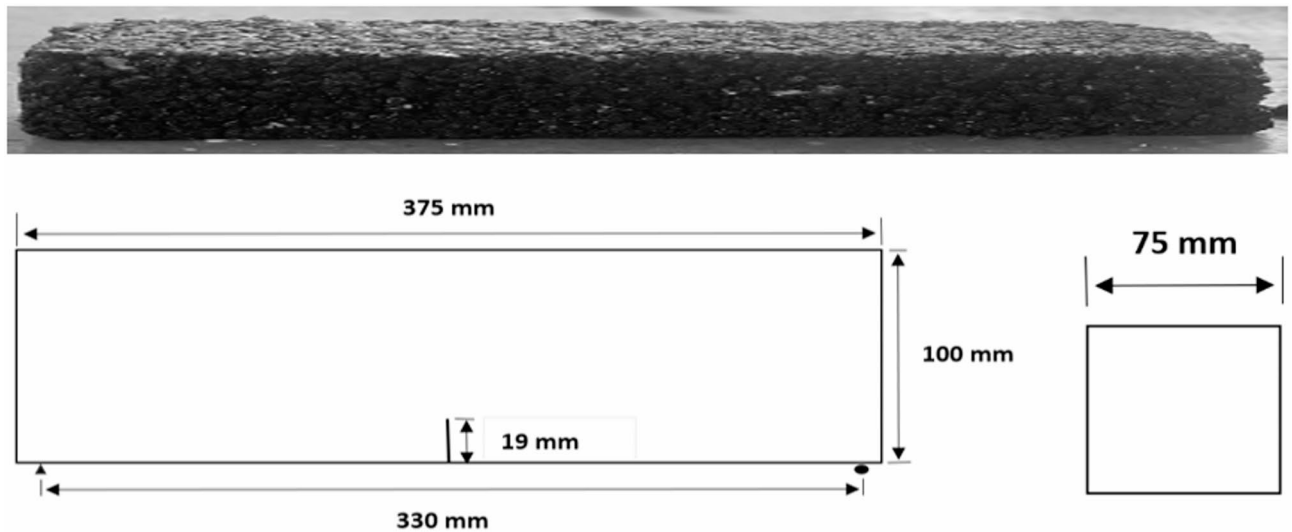


Fig. 2. Single edge notch beam dimensions.



Fig. 3. Single edge notch beam testing.

B gradation specifications. Asphalt Cement (Bitumen) of grade 60–70 was procured from Attock Refinery Limited, Rawalpindi.

To study how temperature affects cracking, the samples were kept in a temperature-controlled chamber for conditioning. Before testing, each beam was kept at the set temperature for 4 h to ensure uniform temperature. The main testing temperature was 20 °C, and tests were performed with a third-point bending setup using a displacement-controlled loading system, as shown in Fig. 3. For each bitumen content level, three specimens were prepared to ensure consistency and allow for reliable averaging of results. A total of five bitumen content levels were tested, resulting in 15 specimens overall (5 bitumen contents \times 3 specimens per content level). During testing, the applied load and corresponding mid-span displacement were continuously recorded until complete failure of the specimen. The load–displacement data were then processed to compute fracture energy (G_f), which represents the energy absorbed by the mixture per unit crack surface area. This metric provided a quantitative measure of the mixture’s resistance to crack initiation and propagation, forming the basis for subsequent finite element validation and the development of surrogate machine learning models.

FEM analyses

For the Finite Element Method (FEM) component of the study, simulations were conducted exclusively at 20 °C to correlate with the experimental data at that temperature. The viscoelastic behavior of the asphalt was modeled using Prony series coefficients. All the inputs and details are tabulated in Table 1.

Parameter type	Property/coefficient	Value	Unit	Temperature (K/°C)	Notes
Material name	–	Python Generated Asphalt Mat	–	–	Defined in input file
Density	ρ	2.4×10^{-9}	tonne/mm ³ (≈ 2400 kg/m ³)	293 K (20 °C)	Standard asphalt mixture density
Elastic modulus	E	1000	MPa	293 K (20 °C)	Long-term modulus
Poisson's ratio	ν	0.3	–	293 K (20 °C)	Typical for asphalt
Viscoelastic (Prony series)	g_1	0.022834	–	–	Time-domain coefficients
	k_1	0.000969	–	–	
	τ_1	0.02007	s	–	
	g_2	0.022945	–	–	
	k_2	0.002201	–	–	
	τ_2	0.045604	s	–	
	g_3	0.023056	–	–	
	k_3	0.003433	–	–	
	τ_3	0.071138	s	–	
	g_4	0.023167	–	–	
	k_4	0.004666	–	–	
	τ_4	0.096673	s	–	
	g_5	0.023278	–	–	
	k_5	0.005898	–	–	
	τ_5	0.122207	s	–	
	g_6	0.023389	–	–	
	k_6	0.007131	–	–	
	τ_6	0.147741	s	–	
	g_7	0.0235	–	–	
	k_7	0.008363	–	–	
τ_7	0.173275	s	–		
g_8	0.023612	–	–		
k_8	0.009595	–	–		
τ_8	0.198809	s	–		
g_9	0.023723	–	–		
k_9	0.010828	–	–		
τ_9	0.224344	s	–		
g_{10}	0.023834	–	–		
k_{10}	0.01206	–	–		
τ_{10}	0.249878	s	–		
Physical constants	Absolute zero reference	–273.15	°C	–	Defined in input file

Table 1. Material properties and constants used in ABAQUS model.

The beam geometry, including the single-edge notch, was first created in Rhinoceros software and subsequently imported into Abaqus/CAE. Within Abaqus, the material properties were assigned, and boundary conditions were established to replicate a third-point loading test setup. A displacement-controlled analysis was performed by applying a 5 mm displacement at the loading points. A comprehensive mesh sensitivity analysis was conducted prior to the final simulations in which five global seed sizes, that are 15 mm, 9 mm, 8 mm, 6 mm, and 5 mm were tested. The comparison was based on the force–displacement curves obtained from the SENB simulations. The corresponding curves to the 5 mm and 6 mm mesh, as shown in Fig. 4, were nearly identical in both peak load and overall curve shape, indicating mesh-independent behavior beyond this refinement level. Consequently, a 5 mm global mesh size was selected for all subsequent analyses as it provided sufficient accuracy with an optimal computational cost. A meshed model is shown in Fig. 5 for visualization purpose.

Following the FEM simulations, the focus shifted to the fracture mechanics and machine learning (ML) phase of the study. The force-displacement data and the evolution of stress fields from the Abaqus models were extracted to calculate key fracture parameters, specifically the fracture energy. This computationally derived fracture energy was subsequently utilized for two primary purposes, that are, validation through comparison with experimentally obtained values, and to serve as the target variable for developing a surrogate model via machine learning for the data set downloaded from Mendeley website (<https://data.mendeley.com/datasets/yb4brz3sdx/3>).

Interpretation of correlation matrix (w.r.t ITSM20)

Before starting machine learning modeling, the correlation analysis was performed which showed that ITSM20 is strongly related to stability which confirms the relationship between stiffness and load bearing capacity.

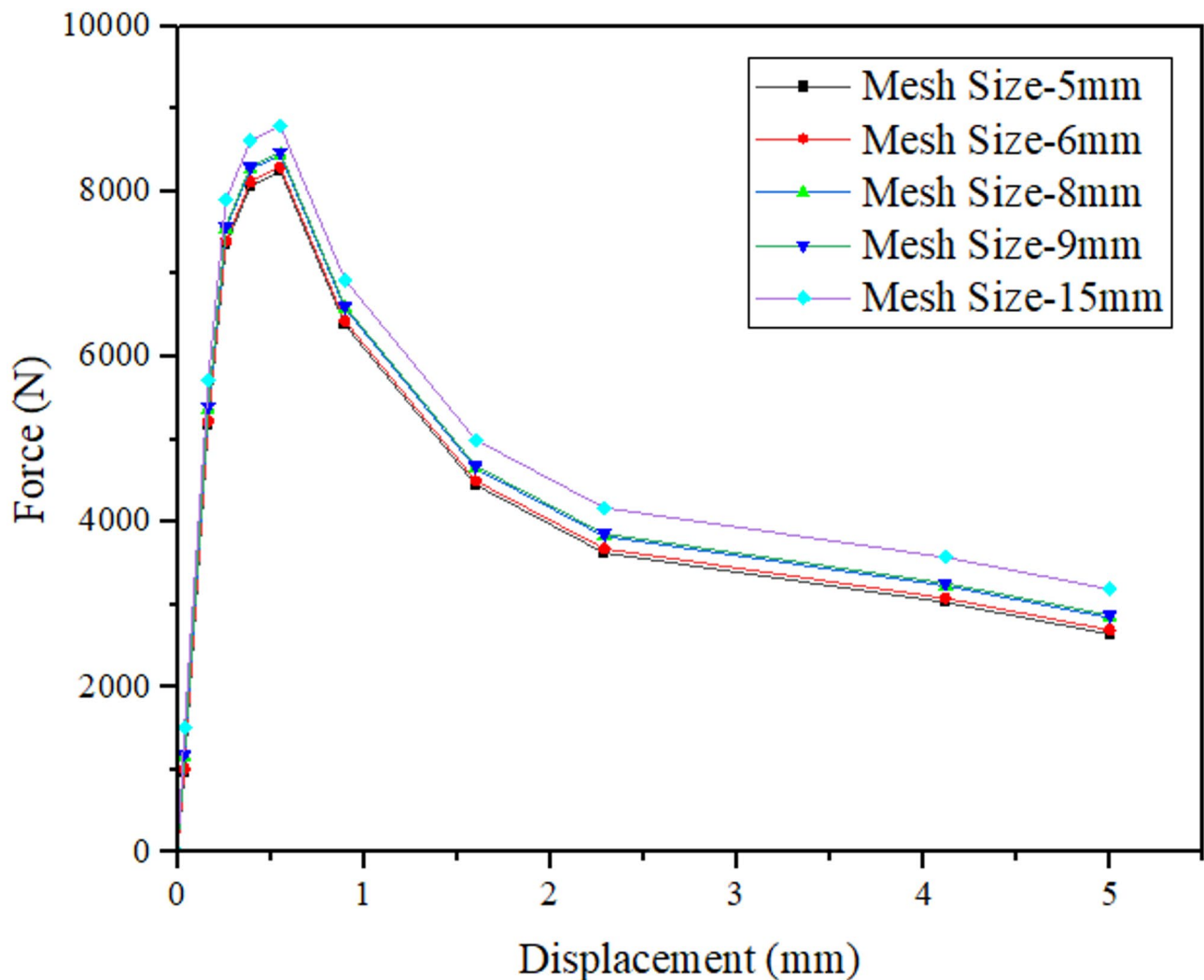


Fig. 4. Force–displacement curve comparison for different mesh densities (Mesh sensitivity study showing overlapping curves for 5 mm and 6 mm meshes, confirming mesh-independent behavior).

Positive correlations with maximum specific gravity and viscosity suggest that dense aggregate packing and binder stiffness enhance mixture rigidity in resisting the load, which was the key parameter in the experimental program as well. Stability to flow ratio also increases with stiffness which points to higher brittleness in stiffer mixtures, which is opposite of experimental program. In contrast asphalt content and effective asphalt content are negatively correlated with ITSM20 reflecting the tradeoff between binder richness and stiffness where richer mixtures are softer but more ductile, as observed in experimental program. Flow also shows a weak negative link with stiffness supporting the idea that more deformable mixtures absorb more energy but resist less load. Overall, the results confirm that stiffness and stability govern toughness while binder content influences fracture energy and ductility. All correlation coefficients are shown in Fig. 6. Table 2 presents the Pearson correlation matrix p-values showing the relationships among key asphalt mixture parameters and the Indirect Tensile Stiffness Modulus at 20 °C (ITSM20).

Machine learning framework

After performing correlation analyses, three machine learning algorithms were implemented to predict fracture related responses from the asphalt mixture dataset, details of which are tabulated in Table 3. In the machine learning framework, the predictive models were trained using a comprehensive set of mixture design, physical, mechanical, and gradation parameters as input features, namely viscosity (Vis), asphalt content (AC), maximum theoretical specific gravity (Gmm), effective asphalt content (EffAC), air voids (Va), unit weight (UWt), stability (Stab), flow value (Flow), stability-to-flow ratio (SFR), percent passing sieve #200 (P200), percent retained on sieve #4 (P4), percent retained on sieve #3/8 (P38), and the coarse-to-fine ratio (CF). These inputs collectively capture the effects of binder rheology, mixture volumetrics, and aggregate structure on mechanical response. The target output for all machine learning models was the Indirect Tensile Stiffness Modulus at 20 °C (ITSM20), which was selected as the primary response variable due to its relevance in characterizing mixture stiffness under service conditions. No models were trained using data at 30 °C. Three algorithms such as Linear Regression,

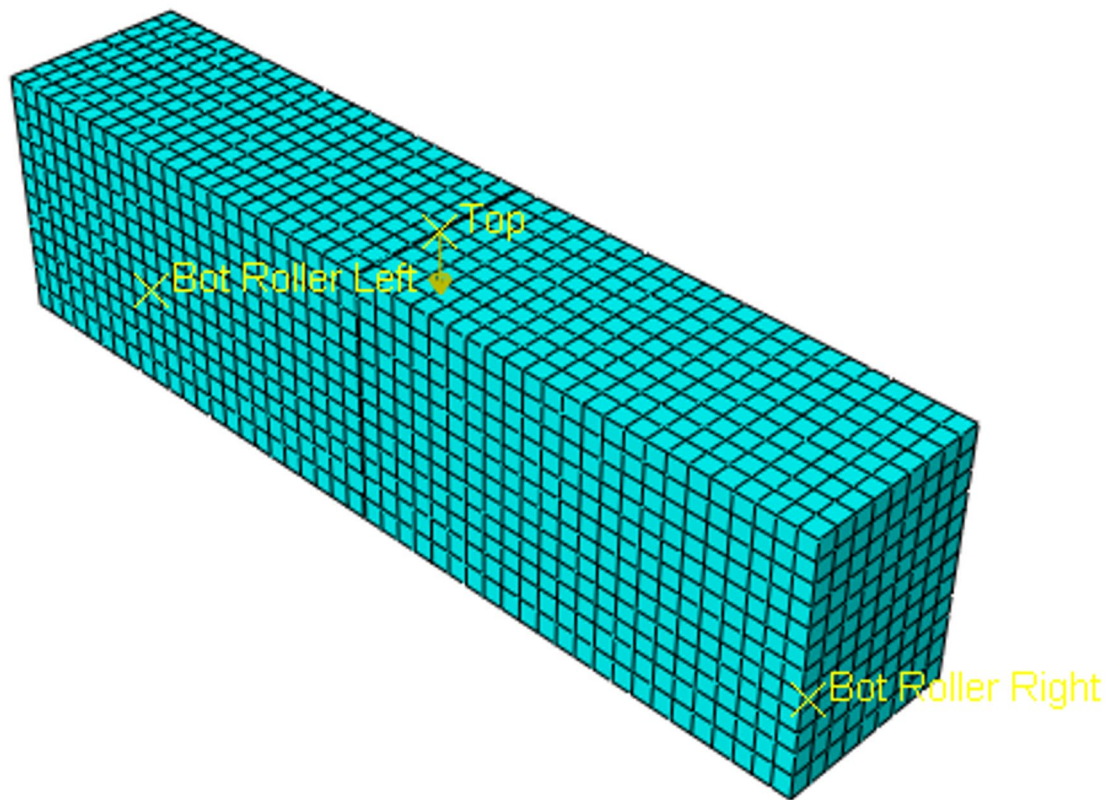


Fig. 5. Meshed ABAQUS model.

Gradient Boosting, and AdaBoost were evaluated using this same input–output structure across multiple cross-validation folds. Gradient Boosting was applied using scikit learn with 100 trees, a learning rate of 0.1, maximum depth of 3 for individual trees, minimum split size of 2, and a full training fraction to ensure replicable performance. AdaBoost was employed with decision tree estimators as the base learner, 50 estimators in total, a learning rate of 1.0, and linear regression loss for continuous target prediction. A standard Linear Regression model without regularization was also used as a baseline due to its interpretability and direct mapping of input parameters to output response. These models were trained under identical conditions and later validated using k fold cross validation to assess robustness and generalization capability.

Cross validation procedure and error analysis

Following The correlation analyses, A k fold cross validation procedure was applied to check the effectiveness of the machine learning models. Different fold numbers including 2, 3, 5, 10, and 20 were tested in all the chosen ML algorithms as shown in Table 4, in order to examine the effect of fold selection on the stability of the performance metrics. This approach ensured that the models were assessed under varying validation schemes and reduced the risk of overfitting to a specific data split. Figure 7 illustrates a cross-validation-based error analysis of three machine learning models across four key metrics (MSE, RMSE, MAE, and R^2) as the number of folds varies from 2.5 to 20. Both Linear Regression and Gradient Boosting were superior models, with Gradient Boosting providing a slight edge in minimizing absolute error at higher fold counts, while AdaBoost was the least suitable choice. The 10-fold cross-validation was finally adopted, as it provided the most consistent R^2 and error metrics across models, ensuring a balanced and reliable evaluation framework.

Surrogate fracture parameters

After selection of machine learning algorithms, surrogate fracture parameters were defined based on key mixture properties from the dataset. These parameters integrate stability, flow, and stiffness modulus to represent fracture energy in a physically meaningful and dimensionally consistent manner. A characteristic beam dimension (k) is incorporated as a scaling factor to relate the surrogate parameter to single-edge notch beam mechanics based on pure novelty. This formulation allows estimation of fracture energy for each dataset sample without performing full experimental tests thus bridging the gap between observed material behavior and predictive modeling with machine learning modeling. The surrogate parameters in this study, serve as target responses for the machine learning models, ensuring that predictions remain grounded in interpretable material behavior observed in experimental program, while enabling rapid, reliable assessment of fracture performance across different asphalt mixtures. This approach adopted in this study, provides a novel, hybrid framework that combines experimental work performed, numerical simulation done, and data-driven insights for practical pavement design and mixture optimization.

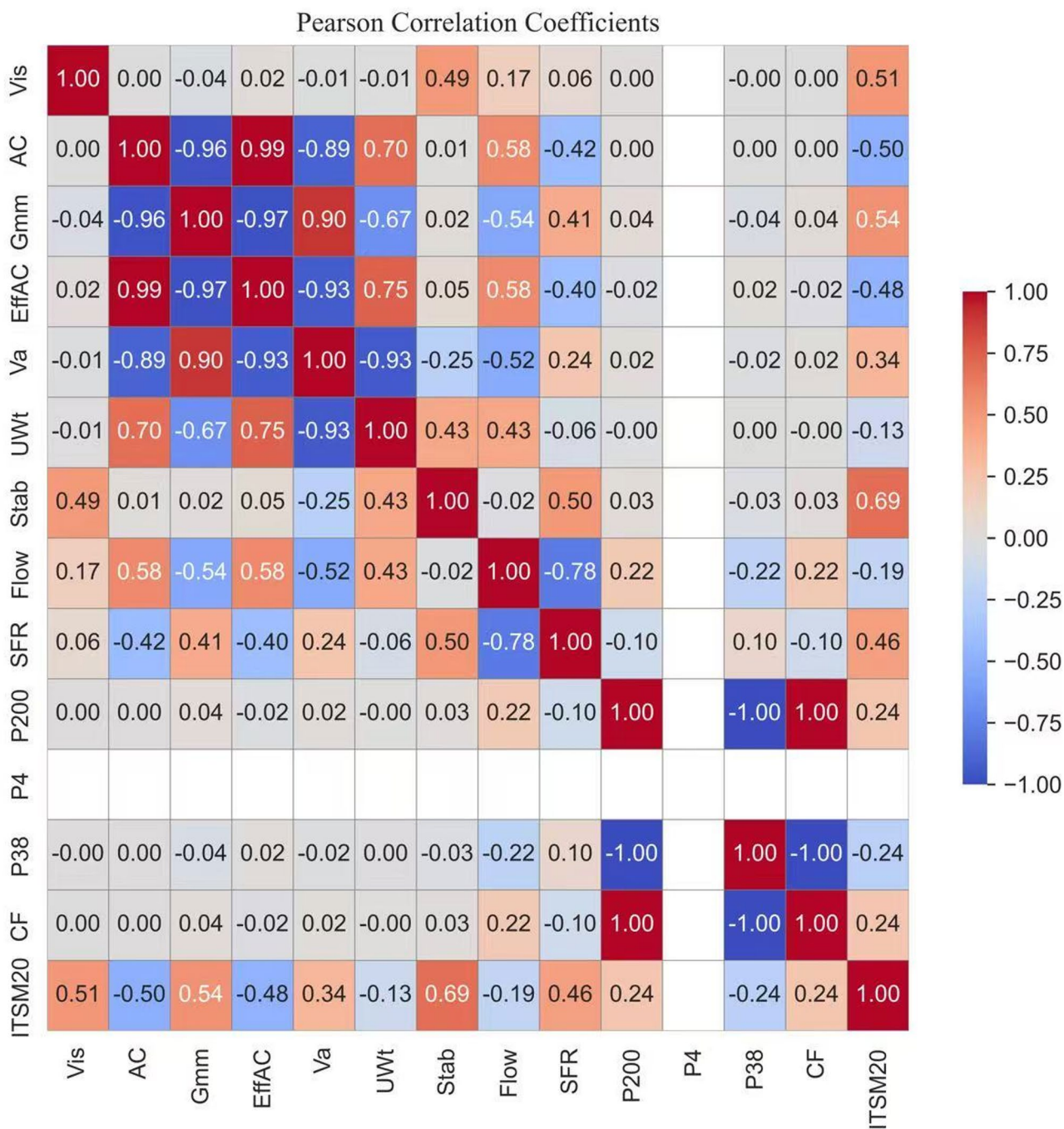


Fig. 6. Pearson correlation.

Discussion

Load–displacement behavior of FEM and experimental result

After completing the experimental program and finite element analyses, the comparison between the finite element model (shown in Fig. 5) and the experimental single edge notched beam (Shown in Fig. 3) results showed good agreement in terms of overall load–displacement behavior as shown in Fig. 9. Both approaches captured the initial linear response followed by gradual softening after peak load, which is characteristic of quasi brittle fracture in asphalt mixtures. The FEM predicted a peak load of around 8.3 kN occurring at a mid-span displacement close to 0.5 mm, which closely matched the experimental measurements. The failure mode is shown in Fig. 8 which matches the experimental failure observed in Fig. 3.

After the peak, the load carrying capacity gradually decreased with increasing displacement gradually through solver controls, and the simulation reproduced the tail of the curve with reasonable accuracy, although it exhibited slightly stiffer post peak behavior compared to the experimental beam as shown in Fig. 9. This

	Vis	AC	Gmm	EffAC	Va	UWt	Stab	Flow	SFR	P200	P4	P38	CF	ITSM20
Vis	0.00	1.00	0.68	0.79	0.88	0.94	0.00	0.05	0.47	1.00		1.00	1.00	0.00
AC	1.00	0.00	0.00	0.00	0.00	0.00	0.90	0.00	0.00	1.00		1.00	1.00	0.00
Gmm	0.68	0.00	0.00	0.00	0.00	0.00	0.85	0.00	0.00	0.68		0.68	0.68	0.00
EffAC	0.79	0.00	0.00	0.00	0.00	0.00	0.57	0.00	0.00	0.81		0.81	0.81	0.00
Va	0.88	0.00	0.00	0.00	0.00	0.00	0.00	0.00	0.00	0.83		0.83	0.83	0.00
UWt	0.94	0.00	0.00	0.00	0.00	0.00	0.00	0.00	0.48	0.96		0.96	0.96	0.14
Stab	0.00	0.90	0.85	0.57	0.00	0.00	0.00	0.84	0.00	0.74		0.74	0.74	0.00
Flow	0.05	0.00	0.00	0.00	0.00	0.00	0.84	0.00	0.00	0.01		0.01	0.01	0.03
SFR	0.47	0.00	0.00	0.00	0.00	0.48	0.00	0.00	0.00	0.27		0.27	0.27	0.00
P200	1.00	1.00	0.68	0.81	0.83	0.96	0.74	0.01	0.27	0.00		0.00	0.00	0.00
P4														
P38	1.00	1.00	0.68	0.81	0.83	0.96	0.74	0.01	0.27	0.00		0.00	0.00	0.00
CF	1.00	1.00	0.68	0.81	0.83	0.96	0.74	0.01	0.27	0.00		0.00	0.00	0.00
ITSM20	0.00	0.00	0.00	0.00	0.00	0.14	0.00	0.03	0.00	0.00		0.00	0.00	0.00

Table 2. Pearson correlations P-values.

Model	Parameter	Value/setting	Description	Data Partitioning
Gradient Boosting	Implementation	scikit-learn	Python library used for model development	10-fold cross-validation (90% train / 10% test per fold)
	Number of trees	100	Total estimators in the ensemble	
	Learning rate	0.1	Step size controlling contribution of each tree	
	Maximum depth	3	Limits complexity of individual trees	
	Minimum samples split	2	Minimum number of samples required to split a node	
	Training fraction	1.0 (full dataset)	Ensures replicable performance	
	Validation method	k-fold cross-validation	Evaluates model robustness and generalization	
AdaBoost	Implementation	scikit-learn	Python library used for model development	10-fold cross-validation (90% train / 10% test per fold)
	Base estimator	Decision Tree Regressor	Weak learner for boosting	
	Number of estimators	50	Total boosting iterations	
	Learning rate	1	Weight applied to each estimator	
	Loss function	Linear regression loss	Appropriate for continuous targets	
	Validation method	k-fold cross-validation	Used for model robustness assessment	
Linear Regression	Implementation	scikit-learn	Python library used for model development	10-fold cross-validation (90% train / 10% test per fold)
	Regularization	None	Standard linear regression without penalty	
	Model type	Ordinary Least Squares (OLS)	Direct mapping between inputs and outputs	
	Validation method	k-fold cross-validation	Consistent with other models for comparison	

Table 3. Machine learning models and their parameter configurations.

difference may be attributed to material heterogeneity and micro cracking in the laboratory specimens that are not fully represented in the numerical model but overall, the close alignment of peak load, stiffness, and softening trend confirmed the reliability of the FEM results.

Experimental program insights

The experimental program provided clear evidence of how asphalt mixture composition influences fracture behavior observed in the testing evaluation. Mixtures with higher stability values exhibited steeper load displacement slopes, reflecting increased stiffness but also a tendency toward brittle failure once the peak capacity of the single notch beam is obtained. Flow values revealed the role of asphalt content, where higher binder levels led to greater deformation capacity and energy absorption, but reduced overall stiffness as shown in Fig. 10. The balance between stability and flow highlighted the classic trade-off between strength and ductility in asphalt systems as visible by the work done highlighted in the Fig. 10. These findings validate the use of surrogate fracture parameters and form the basis for integrating experimental evidence with the FEM predictions and the machine learning framework.

Correlation matrix interpretation

The correlation matrix in Fig. 6, highlighted the dominant role of stiffness modulus at 20 °C in relation to mixture properties. A strong positive correlation with stability (0.695) confirmed that mixtures capable of carrying higher loads also exhibited greater stiffness. Moderate positive links with maximum theoretical specific gravity (0.539)

Model	MSE	RMSE	MAE	MAPE	R2	Number of folds
Linear Regression	188415.38	434.07	335.28	8.64	0.81	2
Gradient Boosting	255052.04	505.03	362.82	9.81	0.75	2
AdaBoost	271540.33	521.10	361.69	9.95	0.73	2
Linear Regression	174700.57	417.97	314.34	8.05	0.83	3
Gradient Boosting	240544.01	490.45	319.16	8.63	0.76	3
AdaBoost	332477.19	576.61	352.92	9.45	0.67	3
Linear Regression	187830.23	433.39	325.02	8.34	0.81	5
Gradient Boosting	177329.34	421.10	258.55	6.70	0.82	5
AdaBoost	264542.67	514.34	311.05	7.98	0.74	5
Linear Regression	187530.01	433.05	326.15	8.33	0.81	10
Gradient Boosting	178226.22	422.17	252.92	6.72	0.82	10
AdaBoost	216532.59	465.33	248.08	6.60	0.79	10
Linear Regression	184273.87	429.27	322.80	8.29	0.82	20
Gradient Boosting	177208.49	420.96	252.26	6.74	0.83	20
AdaBoost	254190.28	504.17	273.72	7.22	0.75	20

Table 4. K-Fold study performed for all ML models.

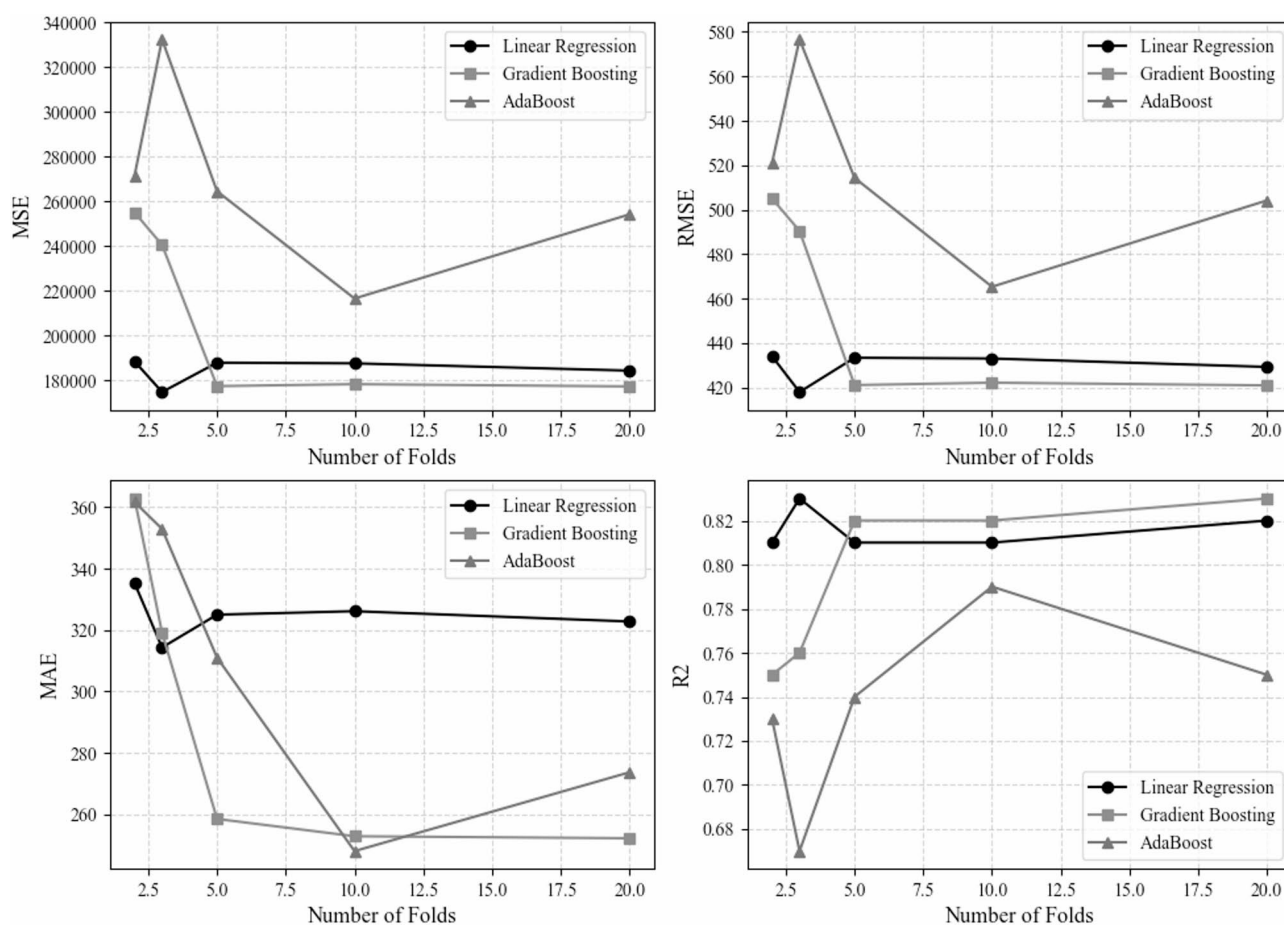


Fig. 7. Error analysis.

and viscosity (0.513) suggested that dense aggregate packing and stiffer binders contribute to higher modulus values. But on the other hand, asphalt content (-0.500) and effective asphalt content (-0.481) showed negative correlations, reflecting the well-known trade off where richer binder mixtures are softer but more ductile. The stability to flow ratio (0.462) also increased with stiffness, indicating more brittle behavior in stiffer mixtures. Air voids (0.342) and fines content (0.241 with P200) properly showed a weaker positive association, while flow (-0.191) and unit weight (-0.127) showed weak negative relationships. Overall, the correlations reinforced that

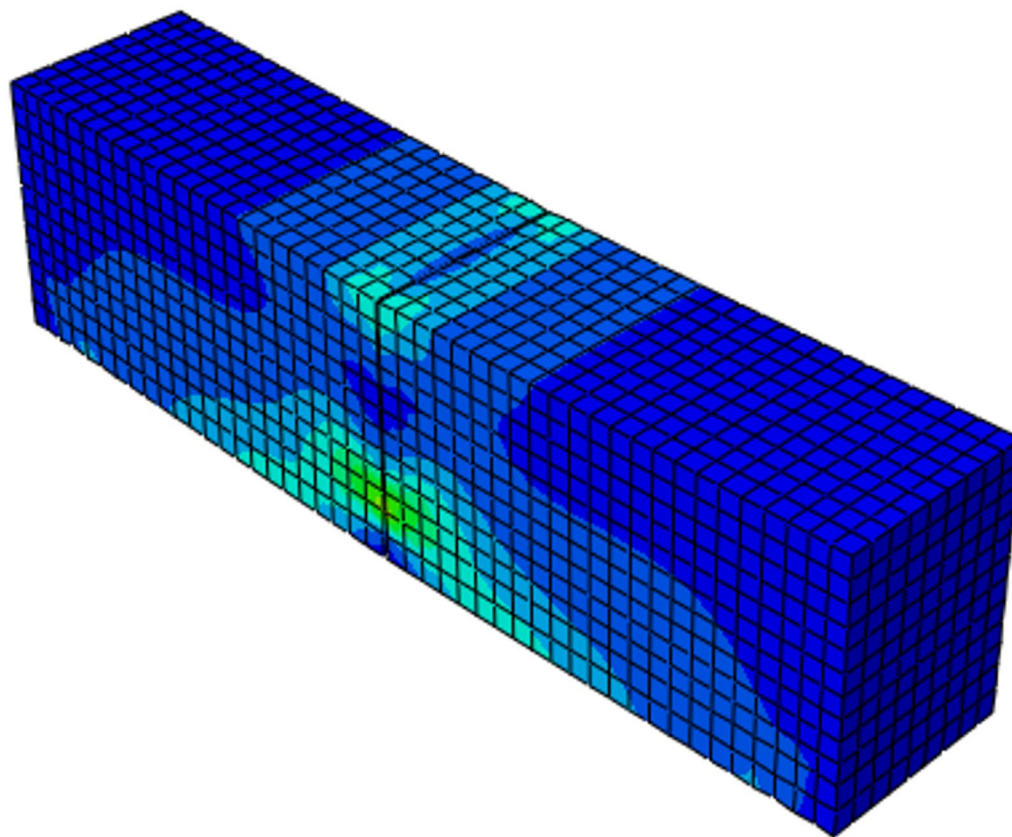


Fig. 8. Deformed shape of asphalt (Contours showing the strain).

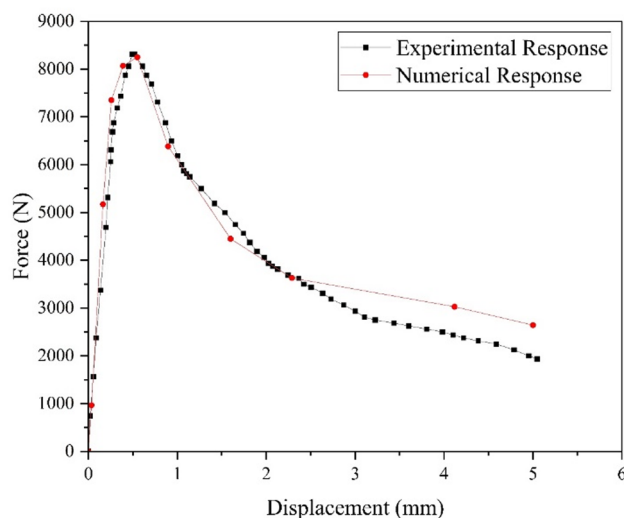


Fig. 9. Comparison of actual vs. numerical response of FD Curve.

stiffness and stability govern load resistance, whereas binder content and flow control the energy absorption capacity of asphalt mixtures.

Surrogate fracture parameters and physical justification

The novelty based surrogate fracture energy (G_f) was formulated, through Python, to capture the fracture behavior of asphalt mixtures using readily same available material properties from the dataset, which were used in the machine learning algorithms. Key parameters are mixture stability, flow, and stiffness modulus were selected based on their established influence on load-bearing capacity, brittleness, and energy dissipation. The

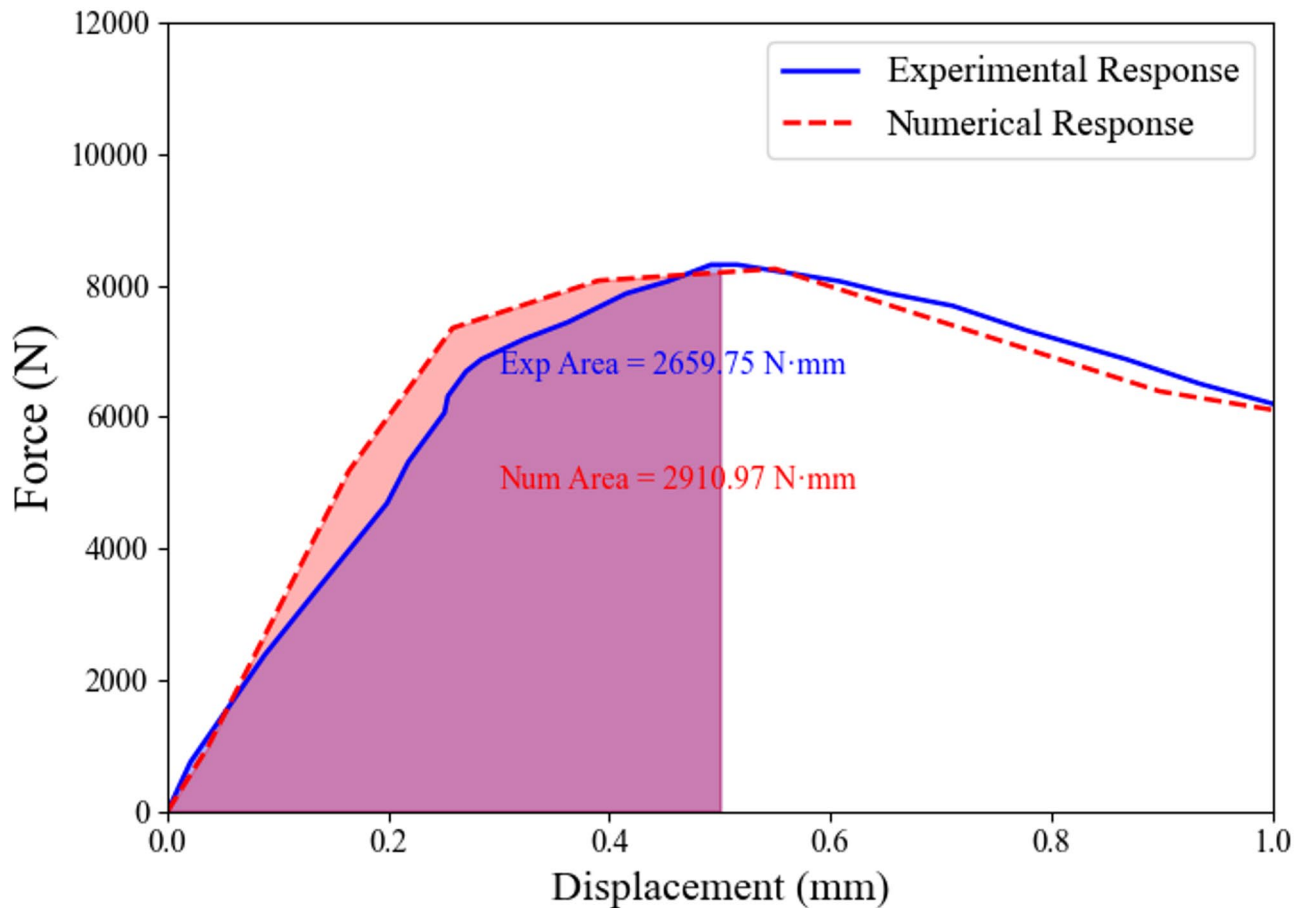


Fig. 10. Fracture energy comparison derived from experimental and numerical load–displacement data.

surrogate formulation is shown in Eq. 1 combines these factors to approximate fracture energy in a dimensionally consistent manner, where the characteristic beam dimension is also included as a physical scaling factor.

$$G_f = k * \{Stab(1 + D) + Flow(ITSM20)\} \quad (1)$$

Where: G_f = surrogate fracture energy [N·mm], k = scaling constant (dimensionless), $Stab$ = mixture stability [N], D = characteristic beam dimension [mm], $Flow$ = mixture flow [mm], $ITSM20$ = stiffness modulus at 20 °C [N/mm²].

This approach is physically justified: higher stability and stiffness increase mixture rigidity and fracture resistance, while flow captures deformability under loading. Figure 11 presents four 3D surface plots (A–D) illustrating the variation of surrogate fracture energy with key mixture parameters across the dataset, enabling visualization of the combined effects of stability, flow, and stiffness modulus.

Table 5 contains the surrogate fracture energy values computed using only $Stab$, $Flow$, $ITSM20$, and the characteristic beam dimension D , along with the corresponding input ranges for these parameters, clearly documenting the domain used for G_f estimation. With these parameters tabulated in Table 5, the surrogate parameter provides an interpretable estimate of fracture energy that aligns with single-edge notch beam mechanics and bridges experimental and computational observations. The proposed surrogated equation is applicable within the calibrated range of the experimental data, representing asphalt mixtures tested at 20 °C, and its extrapolation beyond this range may lead to reduced accuracy.

Machine learning model performance

The predictive performance of the three machine learning models after correlation analyses (tabulated in Table 4) was evaluated across the dataset using $ITSM20$ as the targeted feature. Linear Regression tended to overpredict for lower stiffness values and underpredict for mid-range values, resulting in larger deviations for certain samples. AdaBoost exhibited higher variability, particularly underestimating mid-range stiffness cases. In contrast, Gradient Boosting provided more balanced predictions across the full $ITSM20$ range, closely capturing the trend of the target fracture response while avoiding extreme deviations. The summarization of the comparison of performance is shown in Fig. 12. This consistency suggests that Gradient Boosting is the most reliable model among the three for predicting G_f , offering a best framework for subsequent comparisons with experimental and numerical data.

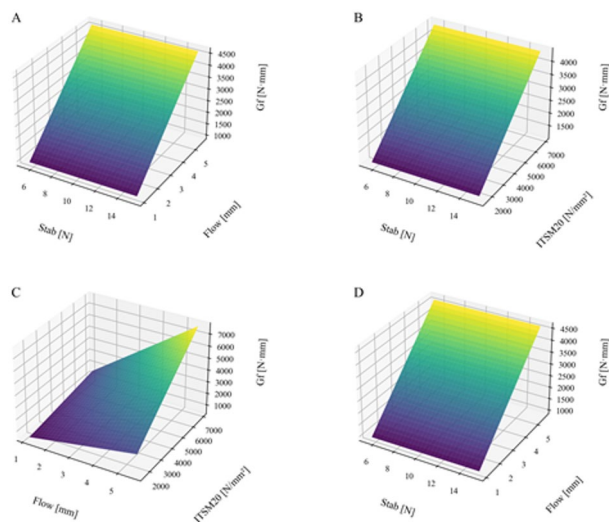


Fig. 11. Variation of surrogate fracture energy with key mixture parameters across the dataset.

Stab	Flow	ITSM20	Gf
9.101029	2.3622	4023	1923.128
10.79594	2.2352	4338	1965.678
7.526036	2.2098	3756	1678.38
5.461002	2.8194	2319	1321.639
8.936968	2.1844	4506	1990.36
12.22918	2.0828	5162	2179.835
11.81969	3.175	4412	2832.765
8.919073	1.8542	3708	1396.22
7.755722	2.1336	3323	1436.812

Table 5. Surrogate fracture energy values computed using only Stab, Flow, ITSM20.

Integration of physics, experiments, and ML

The present study demonstrates a hybrid and novelty-based approach, applied exclusively to baseline asphalt mixtures (National Highway Authority Class B gradation, 60–70 penetration grade bitumen, no additives) by integrating physical modeling, experimental measurements, and machine learning. The surrogate G_f equation, Eq. 1, was derived based on physical reasoning from the single-edge notch beam concept, incorporating key material properties such as stiffness (ITSM20), mixture stability, and flow characteristics. Experimental fracture tests provided reference energy values (2659.75 N-mm), while FEM simulations offered numerical benchmarks (2910.97 N-mm). The machine learning framework then predicted G_f for each dataset sample using the surrogate equation, capturing trends across the domain of input parameters. Comparison of the mean surrogate G_f (2602.26 N-mm) with experimental and numerical results demonstrates excellent agreement within 2% tolerance, validating the integration of physics-guided modeling with data-driven predictions. A chart in Fig. 13 represents the comparison of all integrated results of G_f . This novelty-based approach, adopted in this study, not only ensures dimensional consistency and interpretability but also enables the extrapolation of fracture behavior to untested mixtures, providing a robust framework for performance prediction.

Conclusion and recommendations

Based on extensive research, a physics-guided surrogate equation was developed to accurately estimate the fracture energy (G_f) of asphalt mixtures using key mixture parameters. Based on extensive research, a physics-guided surrogate equation was developed to accurately estimate the fracture energy (G_f) of baseline asphalt mixtures (National Highway Authority Class B gradation, 60–70 penetration grade bitumen, no additives) using key mixture parameters. The proposed approach was validated through experimental testing and Finite Element Method (FEM) simulations, demonstrating strong agreement between predicted and observed results. Correlation and Machine Learning (ML) analyses confirmed that mixture stability, flow, and stiffness modulus (ITSM20) are the most influential parameters governing the fracture response of asphalt mixtures.

In practical engineering terms, the proposed surrogate model provides a cost-effective and time-efficient tool for estimating fracture energy without requiring exhaustive laboratory testing. This makes it suitable for routine quality control, mixture design optimization, and performance-based pavement evaluation in road

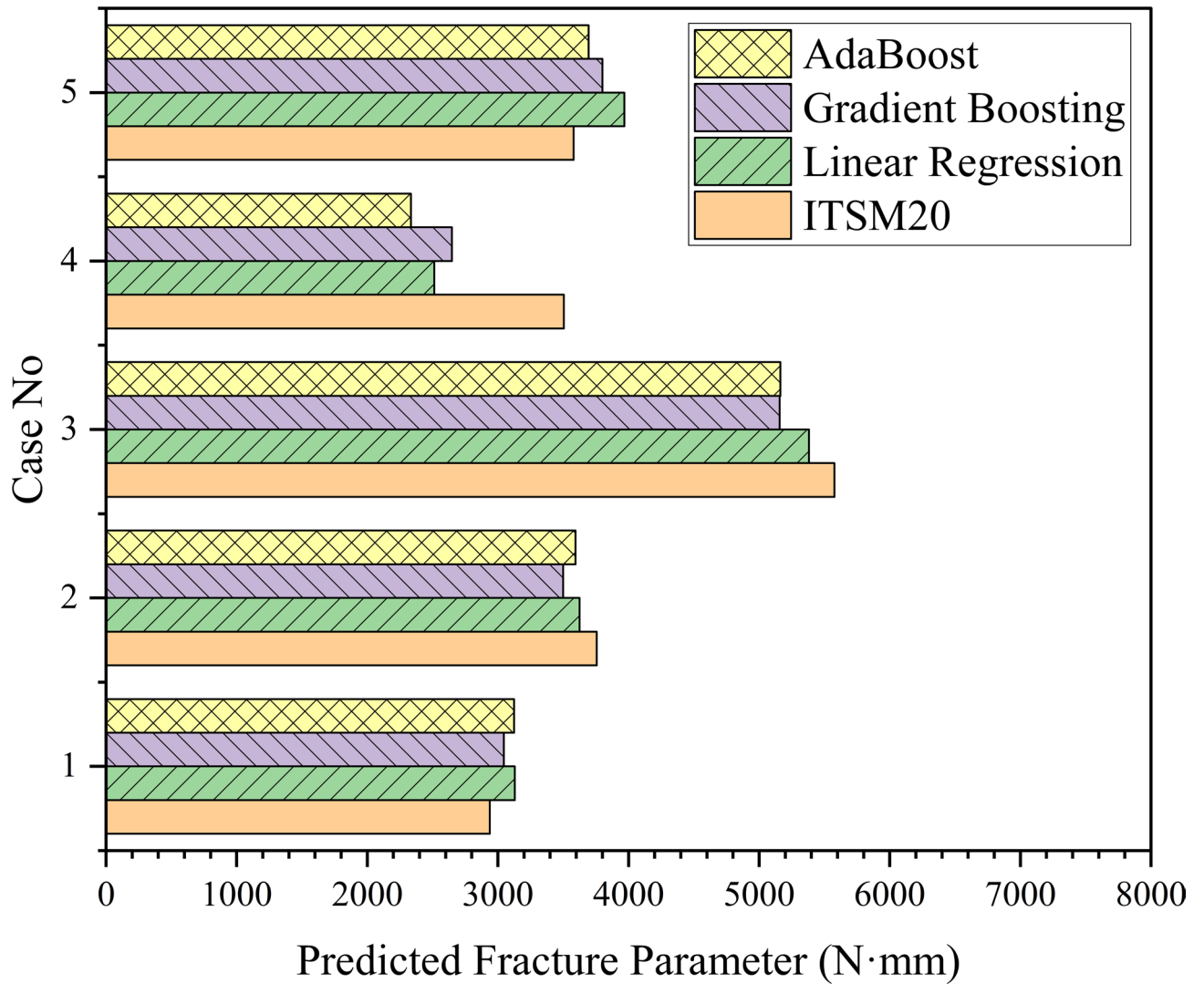


Fig. 12. ML model predictions across dataset samples.

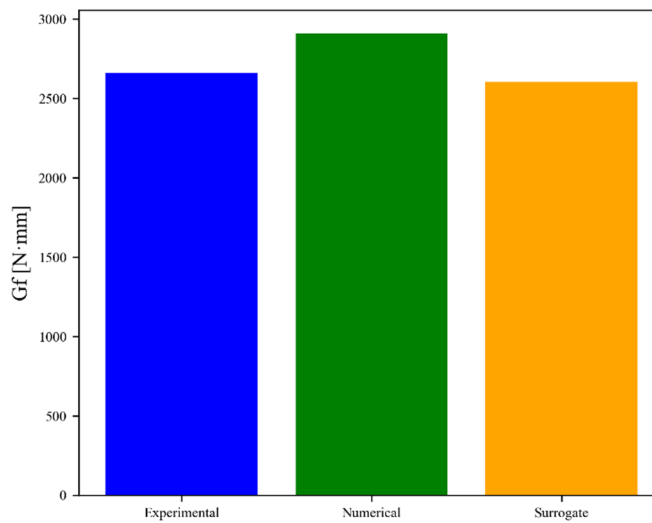


Fig. 13. Comparison of all fracture energies.

construction projects. By predicting fracture resistance at the design stage, engineers can better select bitumen grades, aggregate blends, and binder contents to enhance pavement durability and minimize cracking risks under varying service conditions.

It is recommended that this surrogate fracture approach be further extended to other asphalt mixture types or composite materials exhibiting similar viscoelastic characteristics. Future studies should aim to incorporate temperature- and loading-frequency-dependent effects to improve the model's generality. Moreover, coupling the surrogate model with advanced ML algorithms and field performance databases could support data-driven pavement management systems, enabling more reliable and sustainable infrastructure design.

Data availability

The data presented in this study are available on request from the corresponding author and the data set can also be downloaded from Mendeley website (<https://data.mendeley.com/datasets/yb4brz3sdx/3>)

Received: 15 September 2025; Accepted: 8 December 2025

Published online: 02 March 2026

References

- Horton, M. K. et al. Accelerated data-driven materials science with the materials project. *Nat. Mater.* <https://doi.org/10.1038/S41563-025-02272-0> (2025).
- Sivan, D. et al. Advances in materials informatics: a review. *J. Mater. Sci.* **59** (7), 2602–2643. <https://doi.org/10.1007/S10853-024-09379-W> (Feb. 2024).
- Louie, S. G., Chan, Y. H., da Jornada, F. H., Li, Z. & Qiu, D. Y. Discovering and understanding materials through computation, *Nat Mater*, vol. 20, no. 6, pp. 728–735, Jun. (2021). <https://doi.org/10.1038/S41563-021-01015-1>
- Ramprasad, R., Batra, R., Pilia, G., Mannodi-Kanakkithodi, A. & Kim, C. Machine learning in materials informatics: recent applications and prospects. *NPJ Comput. Mater.* **3** (1). <https://doi.org/10.1038/S41524-017-0056-5> (Dec. 2017).
- Meredig, B. Industrial materials informatics: analyzing large-scale data to solve applied problems in R&D, manufacturing, and supply chain. *Curr. Opin. Solid State Mater. Sci.* **21** (3), 159–166. <https://doi.org/10.1016/J.COSSMS.2017.01.003> (Jun. 2017).
- Bhatt, P., Singh, N. & Chaudhary, S. Potential of machine learning algorithms in material science: predictions in Design, Properties, and applications of novel functional materials. *Mach. Learn. Adv. Funct. Mater.* 75–94. https://doi.org/10.1007/978-981-99-0393-1_4 (Jan. 2023).
- Badini, S., Regondi, S. & Pugliese, R. Unleashing the power of artificial intelligence in materials design. *Materials* **16** (17). <https://doi.org/10.3390/MA16175927> (Sep. 2023).
- Batra, R., Song, L. & Ramprasad, R. Emerging materials intelligence ecosystems propelled by machine learning, *Nat Rev Mater*, vol. 6, no. 8, pp. 655–678, Aug. (2021). <https://doi.org/10.1038/S41578-020-00255-Y>
- Zivic, F., Malisic, A. K., Grujovic, N., Stojanovic, B. & Ivanovic, M. Materials informatics: A review of AI and machine learning tools, platforms, data repositories, and applications to architected porous materials. *Mater. Today Commun.* **48**, 113525. <https://doi.org/10.1016/J.MTCOMM.2025.113525> (Sep. 2025).
- Li, P., Nian, T. & Ma, K. Fracture theory and crack propagation test of asphalt mixture Pre-Notched beam based on weight function method. *J. Highway Transp. Res. Dev. (English Edition)*. **11** (1), 7–13. <https://doi.org/10.1061/JHTRCQ.0000544> (Mar. 2017).
- Ma, Y. et al. Development of a cyclic semi-circular bending test protocol to characterize fatigue cracking of asphalt mixture at intermediate temperature, *Constr Build Mater*, vol. 443, Sep. (2024). <https://doi.org/10.1016/J.CONBUILDMAT.2024.137669>
- Aliha, M. R. M., Razmi, A. & Mansourian, A. The influence of natural and synthetic fibers on low temperature mixed mode I + II fracture behavior of warm mix asphalt (WMA) materials. *Eng. Fract. Mech.* **182**, 322–336. <https://doi.org/10.1016/j.engfracmech.2017.06.003> (Sep. 2017).
- Cheng, L. et al. Evaluation of the fatigue properties for the long-term service asphalt pavement using the semi-circular bending tests and stereo digital image correlation technique. *Constr. Build. Mater.* **317** <https://doi.org/10.1016/J.CONBUILDMAT.2021.126119> (Jan. 2022).
- Kaseer, F. et al. Development of an index to evaluate the cracking potential of asphalt mixtures using the semi-circular bending test. *Constr. Build. Mater.* **167**, 286–298. <https://doi.org/10.1016/j.conbuildmat.2018.02.014> (Apr. 2018).
- Radeef, H. R. et al. Characterisation of cracking resistance in modified hot mix asphalt under repeated loading using digital image analysis. *Theoret. Appl. Fract. Mech.* **116** <https://doi.org/10.1016/J.TAFMEC.2021.103130> (Dec. 2021).
- Pérez-Jiménez, F., Botella, R., Moon, K. H. & Marasteau, M. Effect of load application rate and temperature on the fracture energy of asphalt mixtures. Fénix and semi-circular bending tests. *Constr. Build. Mater.* **48**, 1067–1071. <https://doi.org/10.1016/j.conbuildmat.2013.07.084> (2013).
- Ameri, M., Mansourian, A., Pirmohammad, S., Aliha, M. R. M. & Ayatollahi, M. R. Mixed mode fracture resistance of asphalt concrete mixtures. *Eng. Fract. Mech.* **93**, 153–167. <https://doi.org/10.1016/j.engfracmech.2012.06.015> (Oct. 2012).
- Pirmohammad, S. & Ayatollahi, M. R. Asphalt concrete resistance against fracture at low temperatures under different modes of loading. *Cold Reg. Sci. Technol.* **110**, 149–159. <https://doi.org/10.1016/j.coldregions.2014.11.001> (Feb. 2015).
- Mansourian, A., Razmi, A. & Razavi, M. Evaluation of fracture resistance of warm mix asphalt containing jute fibers. *Constr. Build. Mater.* **117**, 37–46. <https://doi.org/10.1016/j.conbuildmat.2016.04.128> (Aug. 2016).
- Pirmohammad, S. & Ayatollahi, M. R. Fracture resistance of asphalt concrete under different loading modes and temperature conditions, *Constr Build Mater*, vol. 53, pp. 235–242, Feb. (2014). <https://doi.org/10.1016/j.conbuildmat.2013.11.096>
- Ziari, H., Aliha, M. R. M., Moniri, A. & Saghaei, Y. Crack resistance of hot mix asphalt containing different percentages of reclaimed asphalt pavement and glass fiber. *Constr. Build. Mater.* **230** <https://doi.org/10.1016/J.CONBUILDMAT.2019.117015> (Jan. 2020).
- Aliha, M. R. M. & Fattahi Amirdehi, H. R. Fracture toughness prediction using Weibull statistical method for asphalt mixtures containing different air void contents. *Fatigue Fract. Eng. Mater. Struct.* **40** (1), 55–68. <https://doi.org/10.1111/FFE.12474> (Jan. 2017).
- Ilhame, A., Benaissa, K., Hamza, K., Adil, Z. & Parron-Rubio, M. E. Experimental study on the behavior of cement grout-steel sheet interface under shear forces. *J. Building Pathol. Rehabilitation.* **10** (1). <https://doi.org/10.1007/S41024-025-00565-0> (Jun. 2025).
- Xiao, F., Xiao, X. & Li, J. Low-temperature fracture behavior of railway asphalt concretes under semi-circular bending: experimental and numerical investigation. *Constr. Build. Mater.* **402** <https://doi.org/10.1016/j.conbuildmat.2023.132990> (Oct. 2023).
- Guo, Q. et al. Investigation of the low-temperature properties and cracking resistance of fiber-reinforced asphalt concrete using the DIC technique. *Eng. Fract. Mech.* **229** <https://doi.org/10.1016/j.engfracmech.2020.106951> (Apr. 2020).
- Jiang-san, H., Lan, W. & Xin, L. Anti-fatigue performance of warm-mixed rubber powder modified asphalt mixture based on the DIC technique. *Constr. Build. Mater.* **335** <https://doi.org/10.1016/j.conbuildmat.2022.127489> (Jun. 2022).
- Shen, Z., Wang, S., Hu, Z. & Zhao, X. Research on Crack Resistance of Foamed Rubber Asphalt Cold Recycled Mixtures Based on Semi-Circular Bending Test, *Materials*, vol. 18, no. 12, Jun. (2025). <https://doi.org/10.3390/MA18122684>

28. Xu, W. et al. Nonlinear rheological response and fatigue performance of aged composited high viscosity modified asphalt (CHVMA) under large strain amplitude. *Constr. Build. Mater.* **451** <https://doi.org/10.1016/j.conbuildmat.2024.138881> (Nov. 2024).
29. Liang, H. et al. Influence of gradation composition on crack evolution of stone mastic asphalt based on digital image processing. *Theoret. Appl. Fract. Mech.* **136** <https://doi.org/10.1016/j.tafmec.2025.104848> (Apr. 2025).
30. Yuan, F. et al. Full-field measurement and fracture and fatigue characterizations of asphalt concrete based on the SCB test and stereo-DIC. *Eng. Fract. Mech.* **235** <https://doi.org/10.1016/j.engfracmech.2020.107127> (Aug. 2020).
31. Chen, B. et al. Design and construction control of warm mix epoxy asphalt mixture with low epoxy content for service area pavements. *Buildings* **15** (10). <https://doi.org/10.3390/BUILDINGS15101673> (May 2025).
32. Ren, H. et al. Evaluation of fracture behavior in asphalt concrete through the combination of semi-circular bending test and digital image correlation technology. *Constr. Build. Mater.* **451**, 138854. <https://doi.org/10.1016/j.conbuildmat.2024.138854> (Nov. 2024).
33. Ji, J. et al. Study on mechanical properties of curved prestressed BFRP bars for future application in PCCP. *Constr. Build. Mater.* **451** <https://doi.org/10.1016/j.conbuildmat.2024.138873> (Nov. 2024).

Acknowledgements

The authors gratefully acknowledge the availability of the dataset on Mendeley Data and the open research community for providing accessible resources that enable methodological innovation in asphalt pavement research.

Author contributions

Manzoor Elahi: conceptualization, methodology, data curation, software, validation, formal analysis, investigation, writing—original draft. Rawid Khan: conceptualization, methodology, validation, writing—review and editing, supervision. Tufail Mabood: methodology, writing—review and editing, resources, investigation, formal analysis. Muhammad Salman Khan: methodology, resources, investigation, validation, writing—review and editing. Awais Ahmed: methodology, data curation, validation, writing—review and editing. Mahmood Ahmad: data curation, methodology, writing—review and editing, resources. Zsolt Tóth: methodology, writing—review and editing, visualization, validation, funding acquisition.

Funding

Open access funding provided by University of Sopron. This article was supported by the RRF-2.1.2-21-2022-00011 project, financed by the Government of Hungary within the framework of the Recovery and Resilience Facility.

Declarations

Competing interests

The authors declare no competing interests.

Additional information

Correspondence and requests for materials should be addressed to M.S.K. or Z.T.

Reprints and permissions information is available at www.nature.com/reprints.

Publisher's note Springer Nature remains neutral with regard to jurisdictional claims in published maps and institutional affiliations.

Open Access This article is licensed under a Creative Commons Attribution 4.0 International License, which permits use, sharing, adaptation, distribution and reproduction in any medium or format, as long as you give appropriate credit to the original author(s) and the source, provide a link to the Creative Commons licence, and indicate if changes were made. The images or other third party material in this article are included in the article's Creative Commons licence, unless indicated otherwise in a credit line to the material. If material is not included in the article's Creative Commons licence and your intended use is not permitted by statutory regulation or exceeds the permitted use, you will need to obtain permission directly from the copyright holder. To view a copy of this licence, visit <http://creativecommons.org/licenses/by/4.0/>.

© The Author(s) 2026